Tracking Operator State Fluctuations in Gene Expression in Single Cells

B. Banerjee,* S. Balasubramanian,* G. Ananthakrishna,[†‡] T. V. Ramakrishnan,[‡] and G. V. Shivashankar*[§]
*National Centre for Biological Sciences, Tata Institute of Fundamental Research, Bangalore, India; [†]Materials Research Centre, [‡]Centre for Condensed Matter Theory, Physics Department, Indian Institute of Science, Bangalore, India; and [§]Raman Research Institute, Bangalore, India

ABSTRACT We report the results of operator state fluctuations in gene expression for the entire bacterial growth cycle, using single-cell analysis and synthetic unregulated and negative-feedback transcription regulatory gene circuits. In the unregulated circuit, during the cell cycle, we observe a crossover from log-normal-to-normal distribution of expressed proteins and an unusual linear dependence of their standard deviation on the mean gene expression levels. With negative-feedback circuits we find the existence of bimodality as the cell cycle progresses. We suggest that such long-tail and bimodal distributions may be used as selection mechanisms in developmental switches and for assigning cell identity.

INTRODUCTION

Gene expression—the transfer of information from DNA to proteins—is sensitive to fluctuations (McAdams and Arkin, 1997; Hasty et al., 2002; Thattai and van Oudenaarden, 2001). The availability of genome sequences, engineered gene circuits, and single-cell analyses provide a new dimension in exploring mechanisms of gene expression in real biological systems (Becskei and Serrano, 2000; Gardner et al., 2000; Elowitz and Leibler, 2000; Rosenfeld et al., 2002; Swain et al., 2002; Kepler and Elston, 2001). These approaches reveal that noise in gene expression arises at the level of transcription (Becskei and Serrano, 2000; Ozbudak et al., 2002) and translation (Ozbudak et al., 2002) with a subtle distinction between intrinsic and extrinsic origins of fluctuations (Elowitz et al., 2002). Such fluctuations and their time evolutions are believed to play a fundamental role in introducing the cell-to-cell variability or phenotypic diversity that is observed during development (Houchmandzadeh et al., 2002; Sternberg and Felix, 1997) and demonstrated in cell survival strategies (van der Woude et al., 1996; Robertson and Meyer, 1992; van de Putte and Goosen, 1992). Hence, the study of the time evolution of noise characteristics in gene expression and its dependence on cell growth phase is expected to provide insight into developmental processes. Despite its importance this topic has not been explored so far in depth. Our work addresses this issue directly, investigating it at the level of transcription.

Transcription regulation is by far the most dominant gene regulatory process. There are different kinds of genetic networks that underlie such regulation. Simple uncoupled gene expressions to complex interregulatory reactions are known to be functional at the transcriptional level, bringing to the regulation some distinctive features. However, the molecular mechanism of any such regulation is the specific DNA-protein interaction—for example, that between the bacterial lac-operator sequence and the lac-repressor protein. Thus the stringency of gene expression is determined by the resulting operator state fluctuations and is specific to the mode of regulation.

In this work, we elucidate the detailed nature and importance of operator state fluctuations through direct single-cell studies, and propose simple models to account for the observations. Our experiments, for the first time, demonstrate that 1), probing model gene circuits with cell-cycle progression provides new insights into the underlying design principle; 2), characteristics of noise during cell-cycle progression have unique features in the distribution of gene expression that have not been observed before; and 3), the cell-cycle progression is crucial in determining noise features that lead to bimodality in the autoregulatory (negative-feedback) circuit.

We use bacterial cells and the lac operator as a model system to elucidate the effect of cell-cycle progression, and thus the metabolic rate, on the time evolution of the operator state noise in transcription regulation. The state of the operator therefore defines the state of transcription (Fig. 1 *A*). Analyzing the distribution of bacterial gene expression under various regulatory conditions we capture the operator state fluctuations and thus look for signatures of phenotypic cell identity during the entire period of cell cycle. The approach for probing operator fluctuations is to make differential measurements of phenotypic noise by changing the repressor strength and the regulatory mechanism involved. Phenotypic noise is measured via the fluorescent reporter gene product concentration per cell in a population. We use the standard deviation of the distribution and its dependence on the mean as a measure of the phenotypic noise in addition to studying the nature of the distributions. These fluctuations are studied by keeping the ratio of the concentration of the repressor molecules to the operator (or promoter) sites either fixed (~0 and 10, unregulated system) or under autoregulatory genetic

Submitted September 16, 2003, and accepted for publication December 30, 2003.

Address reprint requests to G. V. Shivashankar, E-mail: shiva@ncbs.res.in.

0006-3495/04/05/3052/08 $2.00

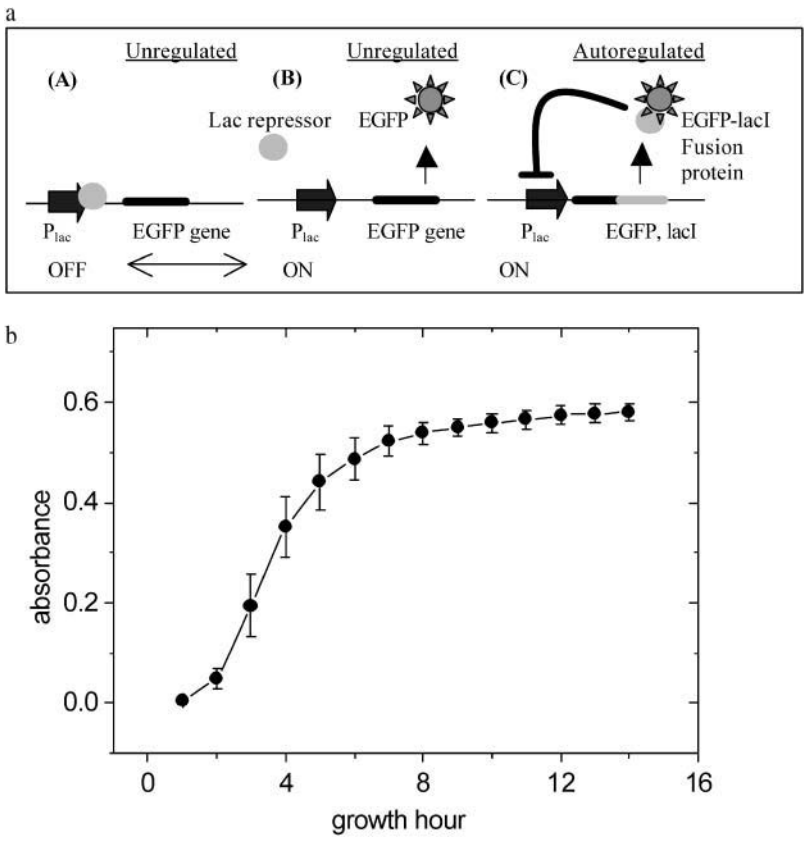

FIGURE 1 (*a*) Schematic of the system used in the experiment. Promoter/operator state is off (*A*) or on (*B* and *C*) depending on repressor bound or unbound to operator sequence. In the autoregulated system (*C*), the repressor is synthesized with the reporter gene as a fused product and thereby represses its own production. (*b*) Plot of absorbance at 600 nm (measurement of cell density) against time. Error bars in the figure represent the variation over the different strains used in the study.

circuits (Fig. 1 *A*). Note that we have used the repressor/promoter (*R*/*P*) ratio in the unregulated circuit merely as a pointer toward the degree of repression. Measurements are done over 20–30 bacterial cell cycles such that all phases of growth are covered (Fig. 1 *B*). This gives information about temporal fluctuations of the operator state and the growth rate-induced tuning of the noise distribution characteristics. We have carried out all the necessary control experiments to check for the functionality of the circuits, and particularly the fusion protein in the autoregulatory system. These are briefly described below (see the Supplementary Materials for details).

EXPERIMENTAL PROCEDURES

Cell culture and flow cytometry

Cells were grown in Luria Broth growth medium and initially cultured overnight before starting the secondary culture. Cells were then collected from the secondary culture at various points in time, spanning all the phases of growth starting from 2 h to 15 h with 1-h intervals (Fig. 1 *B*). Centrifugation was carried out next at 8000 rpm for 6 min and the pellet resuspended in filtered PBS (pH 7.4). Single-cell fluorescence measurements were done on a Becton-Dickinson (San Jose, CA) FACScan flow cytometer with a 488-nm argon excitation laser and a 530/30-emission filter. Each experiment involved signal acquisition from 50,000 cells. The flow rate of the sheath fluid was kept at high, which corresponds to 60 μL $\pm$ 7 μL/min sample through flow cell. Similar gate widths for the side scatter and the enhanced green fluorescent protein (EGFP) fluorescence channels were used in all the experiments. The population average of the protein content per cell as measured above is referred to as the *mean protein content/cell*. The standard deviation is also calculated over the population.

The growth kinetics of all the strains (and their variants) used in the work was first tested by standard optical density measurement. The mean growth curve in Fig. 1 *B* shows similar growth characteristics for all strains. We have also checked and confirmed that there is no dependence of cell morphology (as function of growth hour) on gene expression levels. These observations clearly indicate that there is no inherent difference in either the growth kinetics or the cell morphology over time, which can distort the inferences about the gene expression kinetics.

Construct preparation and promoter efficiency

EGFP gene from pEGFP was cloned into pZERO2 (kanamycin resistance marker, Invitrogen, Carlsbad, CA) to construct a low copy plasmid (colE1 replication origin, ~10 copies/cell). Bacterial strains JM109 (~100 repressor molecules/cell) and MC4100 (0 repressors/cell) were each transformed with low copy plasmids to have two different repressor/promoter ratios (0 and 10). To construct a negative-feedback circuit, lacI gene, coding for lac repressor protein from pMAL-p2, was cloned into the high copy (pUC origin, ~100 copies) pEGFP vector (ampicillin resistance marker, Clontech, Palo Alto, CA) and the cloning was confirmed by sequencing. This vector was then transformed into MC4100 (0 repressors/cell). In all the above constructs, the lac promoter drives the EGFP reporter gene and the expression is regulated by the lac operator sequence.

Multiple copies of the gene and the nature of the medium used (not minimal) make the effective repression lower than expected (Ptashne and Gann, 2002; and see Supplementary Materials). Moreover, the fluorescence is found to increase even into the stationary phase, contrary to what may be naively expected. This is the result of (much stronger) local transcription rate

dominating the rates of dilution (due to cell division) and degradation (see also Supplementary Materials). Here, the strength of the transcription is coming from the multiple gene copies and the choice of the medium (Luria Broth) in which the expression from lac promoter is known to be higher than other minimal mediums (e.g., glucose medium; see Supplementary Materials for details).

Imaging and single-cell fluorescence anisotropy measurements—confirmation of EGFP-lacI fusion protein function

For independent confirmation of the function of the EGFP-lacI fusion protein in the autoregulatory circuits, we have taken images of the cell fluorescence and performed single-cell assays to test the DNA binding property of the protein. Cells were immobilized on a poly-L-lysine-coated glass coverslip and suspended in PBS (pH 7.4) throughout the measurement. An inverted microscope (IX-70, Olympus, Tokyo, Japan) with the right fluorescent filters (Olympus; Chroma, Rockingham, VT) was used in addition to an intensified charge-coupled device (Cascade, Roper Scientific, Tucson, AZ) to take images of the cell fluorescence. Florescence anisotropy $r = (I_{\|} - I_{\perp})/(I_{\|} + 2 \times I_{\perp})$ was measured by exciting the immobilized cell (with 488-nm excitation wavelength, Ar-Ion laser, Spectra-Physics, Mountain View, CA) with polarized light. The fluorescence emission was measured with an analyzer oriented parallel to the excitation ($I_{\|}$) and perpendicular to the excitation ($I_{\perp}$). We use an inverted optical microscope (IX-70 Olympus microscope) with a 1.4 numerical aperture 100× objective lens. The emission fluorescence is detected through a confocal aperture (50-μm pinhole) and avalanche photodetectors (EG&G, Fremont, CA). The details of the experimental setup will be reported elsewhere.

Fig. 2, *A* and *B*, show images of autoregulated cells (*A*) where the fluorescence is due to the fusion protein, and of unregulated cells (*B*) where the fluorescence is due to plain EGFP. The images clearly show the contrast in the localization of the proteins. The fusion protein is located strictly at small polar pockets in the autoregulated cells whereas the EGFP in the unregulated cells is uniformly distributed in the cells. Similar localization of the fusion protein has been reported in the literature (Pogliano et al., 2001; Gordon et al., 1997; Straight et al., 1996) indicating the binding of the protein to the DNA in the cell. This is further confirmed by our single-cell anisotropy measurements performed on the cells. Fluorescence anisotropy is used to characterize rotational mobility of the fluorescing molecules or complexes. The process of binding to DNA is expected to reduce the rotational mobility of the EGFP-lacI protein. Therefore, in vivo measurements of fluorescence anisotropy reveal the mobility of the proteins (EGFP and EGFP-lacI) in their respective environments. The measurements are made on single cells by acquiring the data for 30 s (binning of 0.1 s) at any given point. Each cell is scanned starting at the tip and going inwards. Fig. 2 shows the anisotropy values obtained from such measurements in unregulated and autoregulated cells. In contrast to a uniform anisotropy (~0.2) observed in the unregulated cell (○), the autoregulated cell (●) shows a higher value (~0.33) at the tip, which reduces (to 0.2) as the scan proceeds away from the tip. This demonstrates quantitatively that EGFP-lacI actually binds to DNA (higher anisotropy than free EGFP) and shows that the fusion protein has retained the DNA binding ability of lacI.

RESULTS AND DISCUSSIONS

Unregulated system

The dependence of the mean in gene expression (EGFP photon counts) per cell on cell cycle for repressor strengths $R/P = \sim 0$ (○) and $R/P = \sim 10$ (●) is shown in Fig. 3. The effect of repression on fluctuations in gene expression can be understood by plotting the standard deviation σ as a function of the mean (Fig. 3, *inset*). Interestingly, we find that the standard deviation increases linearly with the mean for both $R/P = \sim 0$ (slope = 0.61) and $R/P = \sim 10$ (slope = 0.52) cases. This finding is rather unusual particularly since for equilibrium fluctuations, the standard deviation varies as square root of the mean, whereas there are no examples of nonequilibrium situations where this linear increase is observed. It is important to note here that this is the first result in which noise in the system has been tracked in real-time during the entire growth phase, and not across different systems under different transcription/translation efficiencies

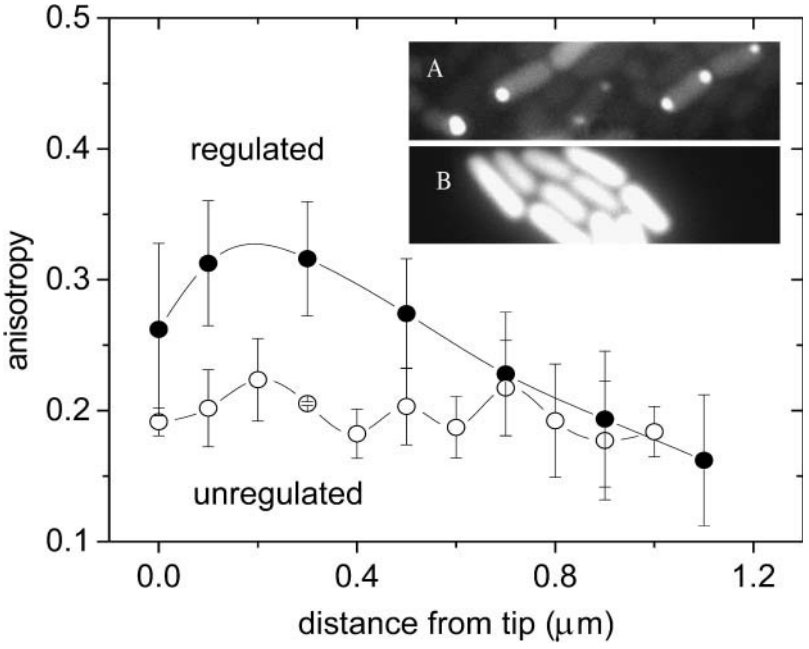

FIGURE 2 Confirmatory tests for DNA binding ability of EGFP-lacI fusion protein: measurement of fluorescence anisotropy while scanning the cells from the tip shows variation in anisotropy in the autoregulated cells and uniform and lower anisotropy values for the unregulated cells. Error bars in autoregulated cells represent the standard deviation in the measurement. For the regulated cells the data shown is averaged over three different experiments, and the error bar represents the variation between these experiments. In the insets, the fluorescence images of cells show localized fluorescence (*A*) for the autoregulated cells (EGFP-lacI protein) and uniform fluorescence (*B*) for unregulated cells (only EGFP).

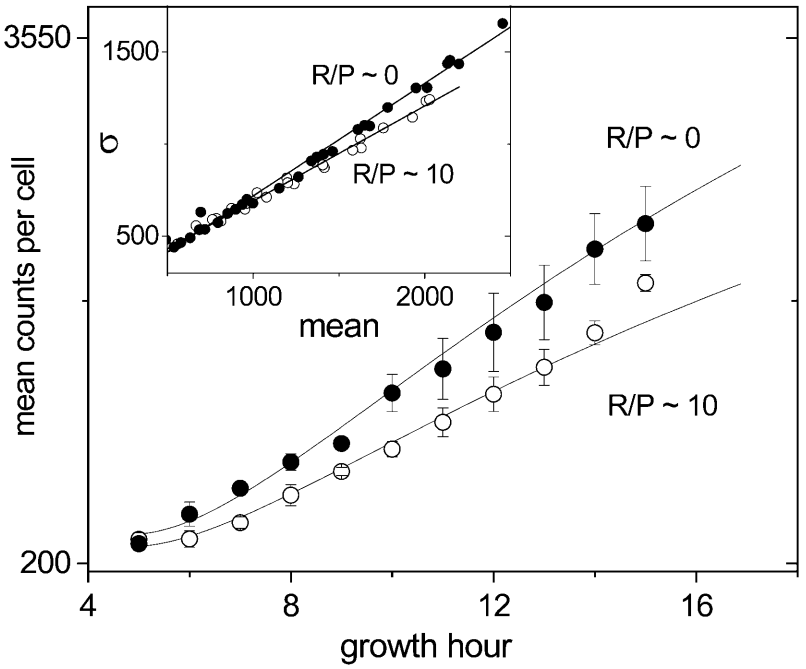

FIGURE 3 Plot of growth of mean protein per cell with time expressed as fluorescence counts in arbitrary units for the unregulated system. Solid lines show the numerical solution for x_f (Eqs. 1 and 2). (*Inset*) Plot of standard deviation σ versus the mean.

as done in previous studies (Ozbudak et al., 2002; Elowitz et al., 2002).

We have simultaneously monitored the time dependence of the probability density of the gene product/cell as function of the growth hour; this is shown in Fig. 4 *A*. The non-Gaussian feature seen at short times crossing over to a Gaussian beyond the mean expression level 750 (Fig. 4 *A*) can be rendered more transparent by plotting the scaled distributions with matching mean and peak heights. This is shown in Fig. 4 *B* along with the fits to log-normal given by $P_{LN}(x) = (A/w\sqrt{\pi/2})$ $\exp(-2(\ln(x/x_c))^2/w^2)$, where $A = 0.003$, $w = 0.905$, and $x_c = 307.0$, and the normal distribution is $P_G(x) = (A'/w\sqrt{\pi/2})\exp(-2(x - x_c)^2/w^2)$, where $A' = 0.557$, $w = 177.8$, and $x_c = 320.3$. The fits are seen to be good. We have also confirmed the fits by checking the Quantile-Quantile plots for log-normal and normal distributions (see Supplementary Materials).

To understand these results we describe the mean kinetics of the unfolded (nonfluorescent) and folded (fluorescent) proteins by the following equations:

$$\dot{x}_u = a\alpha(t) - \gamma(t)x_u - k_f x_u \quad (1)$$

$$\dot{x}_f = k_f x_u - \gamma(t)x_f. \quad (2)$$

Here x_u is the mean concentration/cell of the nonfluorescent protein and x_f that of the fluorescent state of the reporter gene. In each cell x_u is formed at a rate $a\alpha(t)$, and diluted due to cell division at the rate $\gamma(t) = \ln 2/\tau_{celldivision}$, where $\tau_{celldivision}$ is the mean time taken by the cells to divide which itself depends on the bacterial growth phase. At the exponential phase (growth hour 2–5) $\tau_{celldivision} = \sim 25$ min. The cell division time is higher both at the lag (0–2 h) and the stationary phase (6–15 h). k_f is the rate ($k_f = \ln 2/t_{folding\text{-}half\ life}$, where *folding half-life* = 90 min; Tsien, 1998) with which nonfluorescent proteins x_u become fluorescent. The fluorescent protein concentration is also diluted at the same rate as x_u. The protein decay rate was not included, inasmuch as EGFP is stable within the timescale of the experiment (Leveau and Lindow, 2001). The dilution rate is calculated from the experimental data on absorbance versus time of the bacterial culture studied. The protein production rate $a\alpha(t)$ depends on the bacterial growth phase and is taken to be $a\alpha(t) = \gamma(t)^c$.

As can be seen from Fig. 3, the above equations fit (*solid line*) the experimental data (●) for $R/P = \sim 0$ and (○) for $R/P = \sim 10$ quite well. (The values used for the parameters are $c = 0.1$, $x_f = 0.0077$ min^{-1}, and repressor strength, $a_{rep}/a_{unrep} = 0.7$). Since changing average number of repressors changes the average transcription rate and therefore the protein production rate, it is reflected in the parameter a. As we approximate all distributions to be Gaussian using a single parameter $\bar{x}(t)$, identified with the mean gene expression level x_f, we find that the Gaussian form $P(x) = (1/\sqrt{2\pi\sigma_0^2\bar{x}(t)})\exp - (x - \bar{x}(t))/(\sigma_0\bar{x}(t))^2$ fits the experimental distributions over the entire growth curve except at short times where non-Gaussian features are seen. The fact that the Gaussian is a good approximation except at short times can be seen from the χ^2 plot shown in the inset of Fig. 4 *B*. The observation that an increase in repression decreases the ratio of the standard deviation to the mean implies that the repression strength changes the inherent noise.

As the linear dependence of noise on the mean is unusual and appears to arise in biological systems naturally, we have investigated a number of approaches to understand this dependence. Moreover, there has been no stochastic basis for

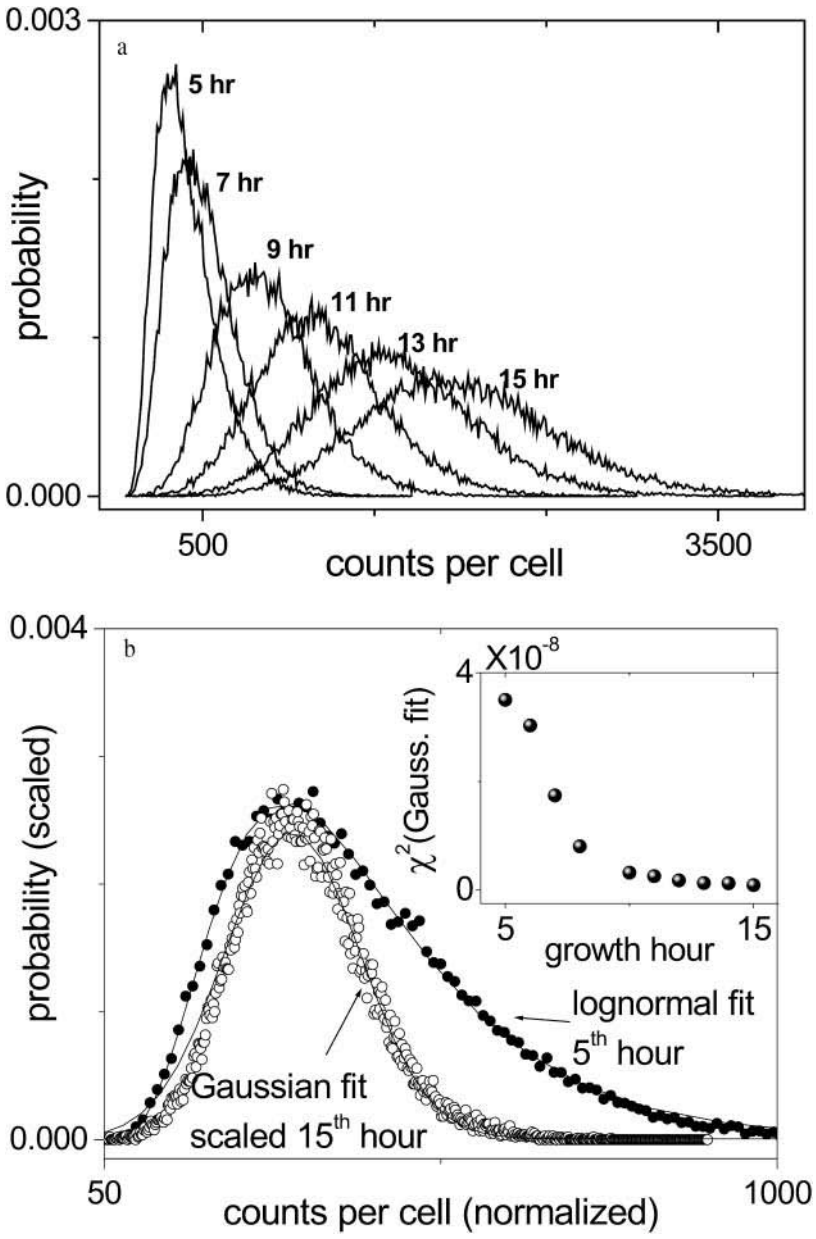

FIGURE 4 (*a*) Plot of single-cell protein distribution in a population ($R/P = \sim 10$) of cells at different growth hours (increasing from *left* to *right*). (*b*) Log-normal and Gaussian curve fits to 5th hour and 15th hour distributions, respectively. Inset shows χ^2 values of the Gaussian fits.

this dependence. Here we present a simple Fokker-Planck-like equation for the physical variable of interest—namely, x, which can be written down by including the time-dependence of (obtained after integrating out) the other variables such as the cell concentration. Such a Fokker-Planck-like equation valid for long timescales would be time-dependent and may be written as

$$\frac{\partial P(x,t)}{\partial t} = -\frac{\partial}{\partial x}(a\alpha(t) - \gamma(t)x)P(x,t) + D\frac{\partial^2}{\partial x^2}xP(x,t). \quad (3)$$

Here $\alpha(t)$ and $\gamma(t)$ are as given in Eq. 2 and D is the noise strength. This choice is equivalent to using the diffusion constant $D(x) = Dx$, arising from a multiplicative process (Risken, 1984). This leads to the equation of motion for the mean and variance of x_f given by $d\bar{x}/dt = a\alpha(t) - \gamma(t)\bar{x}$ and $d\sigma^2/dt = -2\gamma(t)\sigma^2 + 2Dx$, respectively, which in turn gives a linear dependence of σ with x. (Compare the equation for $\bar{x}$ with the sum of Eqs. 1 and 2.) Clearly, the full description requires knowledge of the stochastic evolution of several variables such as the concentration of cells and the fluorescent and nonfluorescent proteins.

Autoregulatory system

To study the repressor noise in a regulated network, we study the mean gene expression level and its distribution as

a function of growth hour with a synthetic negative-feedback circuit. Fig. 5 *A* shows the mean gene expression level per cell (●) as a function of cell cycle having a single maximum due to continuous tuning of the degree of repression. We find that the peak (maximum) occurs at timescales (8 ± 1 cell cycles) close to the maximum growth rate of the cell with a width of 3 ± 1 cell cycles between different experiments, and the maxima is ~100–200 counts per cell. Further, we find that the distribution evolves from a unimodal form (single peak) to a bimodal form (two peaks) as a function of time and remains bimodal. This is shown in Fig. 5 *B* (○, experimental points) and in Fig. 4 *A* in the Supplementary Material. Fig. 4, *B* and *C*, in the Supplementary Materials show other experimental realizations. The two peaks in the probability distributions represent two populations with distinct gene expression levels – repressed and unrepressed. In contrast to the crossover observed from log-normal to normal distributions for the unregulated case, here, the log-normal nature persists all through the growth phase. Indeed, the bimodal distributions can be fitted to the superposition of two log-normal forms (–) as shown in the Fig. 5 *B*. It is clear from Fig. 5 *B* that the bimodality sets in approximately at the time of maximal bacterial growth rate. We find that the realization of unimodal to bimodal transition is very sensitive to experimental initial conditions (see the Supplementary Materials for details). The initial conditions here refer to and are determined by the variability in the gene expression levels at the start of the experiments. A number of initial

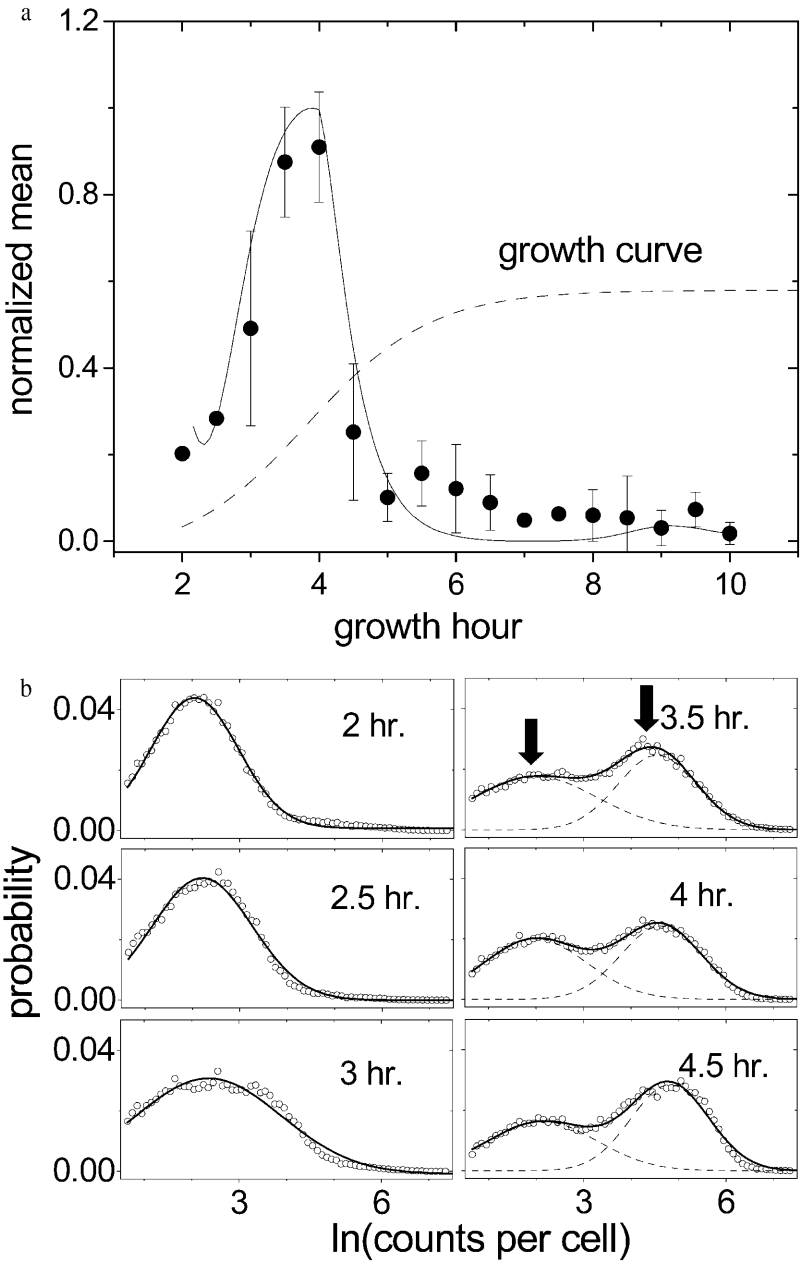

FIGURE 5 (*a*) In the autoregulated system, the mean protein per cell with time shows a peak occurring at timescales when the cells have maximal growth rate. Solid line shows the numerical solution of x_f (Eqs. 4 and 5). (*b*) Single-cell protein concentration distributions for an autoregulated system taken at different growth points show the emergence of bimodality. (*c*) Contour scatter plot of the forward scatter versus side scatter and fluorescence versus side scatter from FACs experiments. Three rows correspond to three time points. (*Autoregulated system*) Plots for the autoregulatory circuit where only the fluorescence channel shows emergence of bimodality; (*Unregulated system*) typical plots for the unregulated system where none of the channels shows any bimodality.

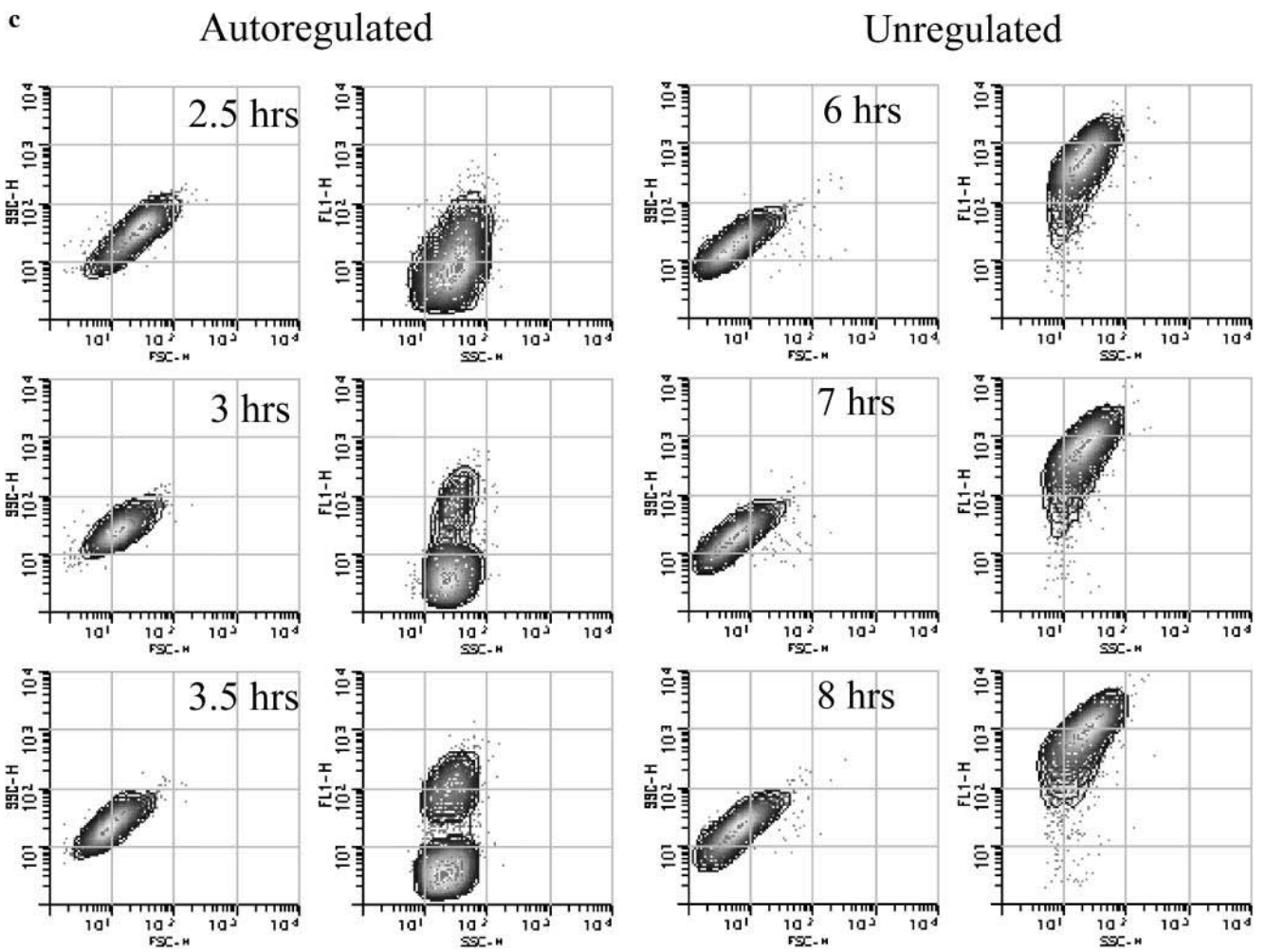

FIGURE 5 Continued.

conditions can be realized experimentally leading to either unimodal or bimodal distributions. Independent of the initial distributions, the major changes in the peak heights occur approximately at the maximal cell growth rate. Also, we have confirmed from our flow cytometry data (Fig. 5 *C*) that wherever bimodality in the gene expression is observed, there is definitely no accompanying bimodality in the population with respect to cell size (or granularity).

To understand the mean kinetics for a negative-feedback system, we consider a modified form of time-delay equation for the nonfluorescent protein x_u (Rosenfeld et al., 2002) and the fluorescent protein x_f,

$$\dot{x}_u = \frac{a\alpha(t)}{\left(1 + \frac{x_u(t-\tau)}{K}\right)} - \gamma(t)x_u - kx_u - k_f x_u \qquad (4)$$

$$\dot{x}_f = k_f x_u - (\gamma(t) + k)x_f, \qquad (5)$$

where K is the binding affinity of the repressor to the operator sequence taken as 10 nM (Rosenfeld et al., 2002), and k is the decay rate of the lac repressor protein, the half-life being taken as 20 min. The value τ is the delay time to complete repression of gene expression from all the promoter sites, which is set to 2 h (~4 cell cycles). The parameters $a\alpha(t)$, $\gamma(t)$, k_f, and c are as defined for Eq. 1. Here we use $c = 0.9$ in $a\alpha(t) = \gamma(t)^c$. Rigorous sensitivity analyses were performed to achieve the optimal values of c,τ for which the least-square fit is best (see Supplementary Materials). As can be seen in Fig. 5 *A*, the solid line fits the experimental data (●) satisfactorily. Our experiments, which display bimodal distributions for a negative-feedback loop, imply the existence of multiple states in the gene expression. Such bimodal behavior in an autorepressive system is indeed possible when there is time delay in the feedback.

CONCLUSIONS

In summary, using simple model systems and synthetic gene circuits, we have captured the effect of operator state

fluctuations in both unregulated and regulated systems. We find that the response (mean, standard deviation, and the nature of the distribution) of the system is directly linked to the growth rate of the bacterial cells. A novel crossover from long-tail distribution (characterized by log-normal) to Gaussian distribution has been observed and may suggest a mechanism for cell diversity as the mean gene expression levels increase with cell cycle. We also find a unique linear dependence of the noise on mean expression level, indicating the coupling of noise features of cell-cycle progression to gene expression kinetics. In the regulated system, the time evolution of the operator state fluctuations leads to bimodal distributions in the expression profile. We find that the onset of bimodality is related to the maximum in the cell division rate. The consequences of time delay as well as competing timescales in the feedback in transcription regulation in negative feedback may lead to such bimodality. It is, however, of interest to test if there is indeed an inherent delayed response in negative feedback in transcription regulation or if it is introduced due to the fusion of reporter proteins on repressor molecules. Our observations of the selection of a population in the long-tail regime with cell-cycle progression may have novel implications in assigning phenotypic cell identity in the developmental context of transcription regulatory switches (Pourquié, 2003). In the early growth phase of an unregulated system, the small number of molecules participating in the gene expression could be the cause of the long-tailed distribution. This may also offer an explanation for the persistence of long-tailed distributions in the regulated case, as the number of participating molecules remains small throughout.

SUPPLEMENTARY MATERIALS

An online supplement to this article can be found by visiting BJ Online at http://www.biophysj.org.

We thank Apurva Sarin for useful discussions.

REFERENCES

Becskei, A., and L. Serrano. 2000. Engineering stability in gene networks by autoregulation. *Nature*. 405:590–593.

Elowitz, M. B., and S. Leibler. 2000. A synthetic oscillatory network of transcriptional regulators. *Nature*. 403:335–338.

Elowitz, M. B., A. J. Levine, E. D. Siggia, and P. S. Swain. 2002. Stochastic gene expression in a single cell. *Science*. 297:1183–1186.

Gardner, T. S., C. R. Cantor, and J. J. Collins. 2000. Construction of genetic toggle switch in *Escherichia coli*. *Nature*. 403:339–342.

Gordon, G. S., D. Sitnikov, C. D. Webb, A. Teleman, A. Straight, R. Losick, A. W. Murray, and A. Wright. 1997. Chromosome and low copy plasmid segregation in *E. coli*: visual evidence for distinct mechanisms. *Cell*. 90:1113–1121.

Hasty, J., D. McMillen, and J. J. Collins. 2002. Engineered gene circuits. *Nature*. 420:224–230.

Houchmandzadeh, B., E. Wieschaus, and S. Leibler. 2002. Establishment of developmental precision and proportions in the early *Drosophila* embryo. *Nature*. 415:798–802.

Kepler, T. B., and T. C. Elston. 2001. Stochasticity in transcriptional regulation: origins, consequences, and mathematical representations. *Biophys. J.* 81:3116–3136.

Leveau, J. H. J., and S. E. Lindow. 2001. Predictive and interpretive simulation of green fluorescent protein expression in reporter bacteria. *J. Bacteriol.* 183:6752–6762.

McAdams, H. H., and A. Arkin. 1997. Stochastic mechanisms in gene expression. *Proc. Natl. Acad. Sci. USA*. 94:814–819.

Ozbudak, E. M., M. Thattai, I. Kurtser, A. D. Grossman, and A. van Oudenaarden. 2002. Regulation of noise in the expression of a single gene. *Nat. Genet*. 31:69–73.

Pogliano, J., T. Q. Ho, Z. Zhong, and D. R. Helsinki. 2001. Multicopy plasmids are clustered and localized in *Escherichia coli*. *Proc. Natl. Acad. Sci. USA*. 98:4486–4491.

Pourquié, O. 2003. The segmentation clock: converting embryonic time into spatial pattern. *Science*. 301:328–330.

Ptashne, M., and M. Gann. 2002. Genes and Signals. Cold Spring Harbor Laboratory Press, New York.

Risken, H. 1984. The Fokker-Planck Equation. Springer-Verlag, Heidelberg, Germany.

Robertson, B. D., and T. F. Meyer. 1992. Genetic variation in pathogenic bacteria. *Trends Genet*. 8:422–427.

Rosenfeld, N., M. B. Elowitz, and U. Alon. 2002. Negative autoregulation speeds the response times of transcription networks. *J. Mol. Biol*. 323:785–793.

Sternberg, P. W., and M. A. Felix. 1997. Evolution of cell lineage. *Curr. Opin. Genet. Dev*. 7:543–550.

Straight, A. F., A. S. Belmont, C. C. Robinett, and A. W. Murray. 1996. GFP tagging of budding yeast chromosomes reveals that protein-protein interactions can mediate sister chromatid cohesion. *Curr. Biol*. 6:1599–1608.

Swain, P. S., M. B. Elowitz, and E. D. Siggia. 2002. Intrinsic and extrinsic contributions to stochasticity in gene expression. *Proc. Natl. Acad. Sci. USA*. 99:12795–12800.

Thattai, M., and A. van Oudenaarden. 2001. Intrinsic noise in gene regulatory networks. *Proc. Natl. Acad. Sci. USA*. 98:8614–8619.

Tsien, R. Y. 1998. The green fluorescent protein. *Annu. Rev. Biochem*. 67:509–544.

van de Putte, P., and N. Goosen. 1992. DNA inversions in phages and bacteria. *Trends Genet*. 8:457–462.

van der Woude, M., B. Braaten, and D. Low. 1996. Epigenetic phase variation of the pap operon in *Escherichia coli*. *Trends Microbiol*. 4:5–9.